ISSN: 2524-1354 (Online), ISSN: 2519-7851 (Print)
Africa Habitat Review Journal
Volume 14 Issue 3 (December 2020)
http://uonjournals.uonbi.ac.ke/ojs/index.php/ahr

Thermal Conditions in Sheet Metal Clad Residential Buildings:
A Case Study of Kiambu County, Kenya

Peter M. Gathirimu*, Charles Kabubo and Patrick Ajwang

Received on 14th July, 2020; Received in revised form 1st August, 2020; Accepted on 15th September, 2020.

Abstract

This research aimed to conduct a field study on sheet metal clad residential buildings with an aim to gather data to determine their thermal comfort, condensation risk and develop a micro-climate predicting model. The geographical area for the study was Uthiru in Kiambu County. The findings of this research document the thermal comfort (and living conditions) of sheet metal clad buildings under normal residential use which are exposed to the same climatic conditions simultaneously. A web-based application software (Thermal Comfort Tool for ASHRAE-55) based on adoptive method of ASHRAE Standard 55-2017 was used to check the compliance on the thermal comfort of the case study buildings. From the temperature and relative humidity data, absolute humidity values and dew point temperatures were calculated thereby determining the level of condensation risk on the buildings. Use was made of Microsoft Windows Excel application to analyze the collected data and to develop a microclimate predicting model. The recommendations are specific to the case study buildings' design adjustments that could be required and recognition for acceptability of the sheet metal clad buildings as worthy to be included in the Kenya Building Code.

Keywords: Absolute humidity, Correlation, Dew point, Relative humidity, Thermal comfort.

INTRODUCTION

The high demand for affordable sustainable residential buildings in Kenya is not being met, and thus the use of galvanized sheet metal houses by local developers for site accommodation, cheap rental housing and private homes has increased. Sheet metal building structures come in different forms in Kenya; first, there is the simplest form constructed of a light wooden frame covered with light gauge galvanized sheet metal; secondly, there is the 'uni-hut' type made of heavy gauge galvanized structural sheet metal; and lastly, there is the shipping container building structure (Republic of Kenya (ROK), 2016). During a sunny day the metal structures transmit a lot of heat internally and during chilly nights they lose heat fast to the external environment (Abrasheva, Senk & Häußling, 2012).

Simple sheet metal clad buildings are used as sheds and barns in the temperate countries and are not considered as shelter for human habitation due to their poor insulation capacity. The simple sheet metal clad building is the most popular in tropical Africa and Kenya in particular where they are used for accommodation in the informal settlements. Studies have shown that in Nairobi alone, 60% of the population lives in the informal settlements (ROK, 2016).

Thermal comfort is a fundamental aspect of indoor environmental quality and is strongly related to occupant satisfaction and energy use in buildings. There are three relevant standards regarding thermal comfort namely; the International Standard ISO 7730 (2005), the European Standard EN 15251 (CEN 2007) and the ASHRAE 55 (2017) (Schiavon, Hoyt & Piccioli, 2019). This research used the adoptive method of ASHRAE 55 (2017) to check the thermal comfort standards of the buildings being studied.

Thermal comfort research using climate chamber methodology permits an independent environmental variable to be manipulated directly while at the same time isolating the dependent

*Corresponding author:
Peter M. Gathirimu, Department of Construction Technology and Built Environment, National Youth Service Engineering Institute, Nrb, Kenya.
Email: pmgathirimu@gmail.com

variable, comfort level, from extraneous influences. Controlled tests in laboratories using climate chambers have been the source of data for professionals of the built environment. Case studies of thermal comfort in the field tend to have greater external validity than laboratory-based methods (Dear, Foo & Leow, 1991).

In Kenya, there is need to research on the level of satisfaction with indoor thermal environment on building users in the tropical highland areas of Africa as available literature is based from studies abroad (Kariuki et al., 2018) This research aimed to study thermal conditions, thermal comfort and humidity conditions of simple galvanized sheet metal clad residential buildings.

THEORY

Effects of solar reflectance on heat gain

Close to the equator, ambient temperatures and solar radiation levels are sufficiently high in locations such that during cold seasons, buildings do not require active heating (Suehrcke, Peterson & Selby, 2008). Surface orientation, solar position and atmospheric conditions influence solar reflectance variation with the spectral and angular distributions of incident sunlight (Levinson, Akbari & Paul, 2010).

Occupants adaptive response to thermal environment

Research has shown that people adjust themselves to maintain and improve their well-being through physiological, psychological and behavioral reactions to environmental stimuli (Han et al., 2007).

Indoor air temperature and humidity effects on comfort

Increased thermal stress at temperatures of 35^0 and a high relative humidity of 75% causes a significant reduction in REM sleep. At lower temperatures (29^0) whether with high relative humidity (75%) or low relative humidity (50%), sleep quality is not affected much. At higher temperatures of 35^0 and a lower relative humidity of 50% sleep quality is not affected much. Hence high temperatures combined with high humidity are disruptive to sleep patterns. Thermal comfort design in buildings aims to attain the most acceptable combination of temperature and humidity levels in a residential building (Okamoto-Mizuno, Mizuno, Michie, Maeda & Iizuka, 1999).

Converting relative humidity to absolute humidity

From the formula in **Equation 1**, temperature (T) is expressed in degrees Celsius, relative humidity (RH) is expressed in %, and *e* is the base of natural logarithms 2.71828 [raised to the power of the contents of the square brackets]. This formula is accurate to within 0.1% over the temperature range -30°C to +35°C (Bolton, 1980).

Calculating the dew point temperature (T_d)

Equation 2 shows a simple calculation that gives an approximation of dew point temperature where the observed temperature and relative humidity are known.

Equation 2:

$$T_d = T - \left(\frac{100-RH}{5}\right)$$

Where T_d is dew point temperature (in degrees Celsius), T is measured temperature and RH is relative humidity (in percent).

This relationship is fairly accurate for relative humidity values above 50% (Lawrence, 2005).

RESEARCH METHODS

This paper presents an investigative research that

Equation 1:

$$\text{Absolute Humidity}\left(\frac{grams}{m^3}\right) = \frac{6.112 \times e\left[\frac{17.67 \times T}{T+243.5}\right] RH \times 2.1674}{(273.15+T)}$$

studied the relationship of the influence of outdoor temperatures/humidity on indoor temperatures/humidity influencing thermal comfort in galvanized sheet metal clad residential buildings. Research location and design were chosen in order to have data that is consistent and reliable and has no bias on effects of a particular geographical location and climatic conditions, and can hence be replicated in any other geographical location. The thermal comfort standard of reference was the ASHRAE Standard 55-2017 and its related web-based application (Thermal Comfort Tool for ASHRAE-55) was used to check the thermal comfort of the case study buildings.

A microclimate predicting model was developed using Microsoft Excel to predict the thermal conditions of the buildings at any given time of the year. A web-based application (Thermal Comfort Tool for ASHRAE-55) based on ASHRAE Standard 55-2017 was used to check the levels of thermal comfort being experienced in the buildings at different times of the day over a 24-hour period. Continuous recording of temperature and humidity data was taken over a period of six months covering the warm and cold seasons.

The study started with two identical buildings of the same size (one occupied and the other vacant) located on the same grounds exposed to the same environment and later on, other buildings were used in the validation process. The floors of the case study sheet metal clad residential houses were made of lightweight concrete. Thermal conductivity decreases with the increment in volume of coarse aggregate since it represents a reduction in the density of concrete (Real, Gomes, Bogas & Ferrer, 2016).

Data loggers were installed in the sitting/kitchen room which had 100% occupancy in the evenings. On site measurements of temperatures and relative humidity were taken for both the indoors and outdoors environments. Data logger 1 was set under the shade away from direct sunlight and wind; data loggers 2 and 3 were set in the case study houses. A laptop with software for operating the data loggers was used to synchronize them and download collected data.

The data collecting instruments (The ELITECH RC-4HC data logger) were calibrated using meteorological data from the Kabete Veterinary Laboratories Meteorological Station which is two kilometers away.

Referring to **Figure 1**, temperatures recorded on the research site (Outdoors temp) were compared with those recorded at the Kabete Veterinary Laboratories Meteorological station (Dry bulb temps) and were shown to have a high positive correlation with a coefficient of determination (R^2) of 0.9193. That means 91.93% of the recorded research site temperature data can relate to that recorded at the nearby Kabete Vet Lab Meteorological Station.

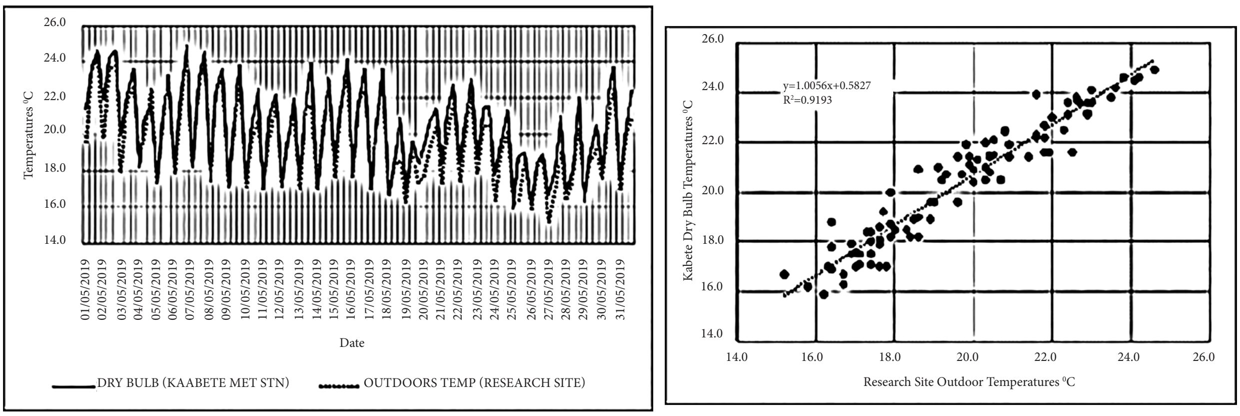

FIGURE 1
Correlation of research site and Kabete Meteorological Station temperature data
Source: Author 2020

The first full month data set was collected on May 2019 for a vacant house (House A) and an identical occupied house (House B). House A represents an ideal house model with no thermal or relative humidity influence of occupants while House B represents a typically occupied house with the occupants free to adapt, influence and control their environment to suit their comfort. By use of recorded data of temperatures and relative humidity values, absolute humidity values were calculated as well as the dew point temperatures for all the case study houses so as to determine their risk of internal condensation formation and when it is likely to occur. The data collected for the month of May 2019 was used to develop several regression models from the two houses (House A data developed Model As and House B data developed Model Bs) by use of Microsoft Excel software.

A full month data set was collected for month of July 2019 which was used to validate the prediction accuracy of the regression Model As and regression Model Bs. The most accurate model was selected and was validated with full month data of August 2019 (Houses B & C) and October 2019 (Houses D & E).

A web-based application (Thermal Comfort Tool for ASHRAE-55) was used for thermal comfort calculations, visualization and compliance checks against standards set by the ASHRAE Standard 55 (2017).

RESULTS AND DISCUSSION

(a) Layout plans and building usage

(i) House A and B

House A was a vacant two roomed house with one entry door and one window. House B was an occupied two roomed house that is identical in layout as House A (**Figure 2a**). Both houses were made of galvanized sheet metal with no internal lining or insulation and covered with a gable roof as shown in **Figure 2b**.

House A was studied in a closed unventilated state as the doors and window remained closed throughout the data collection period. House B was studied in the state of its users' adaptation to their environment. House B was occupied by three adults and three children. Users woke up at 5am to heat bathing water and prepared breakfast for the father and a school going child; 9am breakfast was prepared for the toddlers and the occupants opened the door and window depending on the day's climate; at 12pm lunch was prepared and thereafter people relaxed outside depending on the day's weather; from 6pm laundry was collected from outside and preparation of supper commenced at 7pm; on weekdays the door remained open and the window shut when a gas stove is used for cooking until 9pm (on weekends, the door and window would remain open when a charcoal stove was used until they finished cooking and remove the stove outside at 9pm); thereafter the occupants relax in the sitting area until 11pm then they went to sleep. One adult slept in the sitting area together with the toddlers while the couple slept in the bedroom.

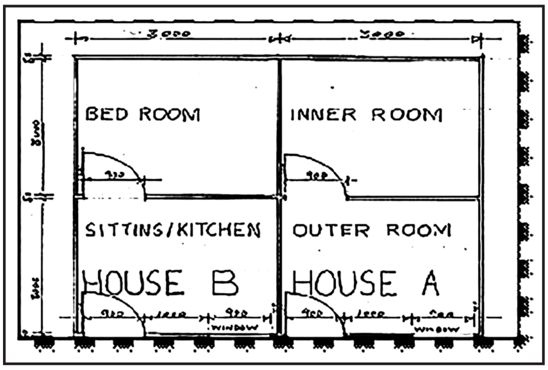

FIGURE 2a
House A & B layout plans
Source: Author 2020

FIGURE 2b
House A & B pictorial view
Source: Author 2020

(ii) House C

House C was an occupied three roomed self-contained house (**Figures 3a** and **3b**) with a family of four: a mother and her three grown-up children.

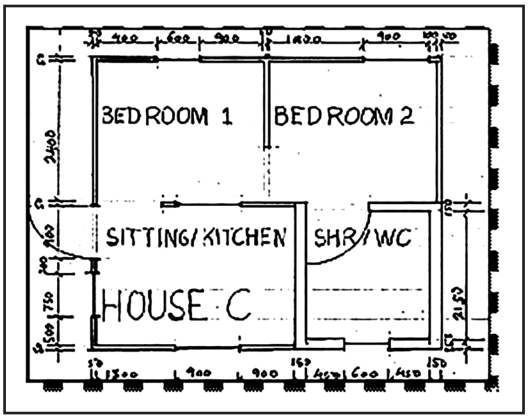

FIGURE 3a
House C layout plan
Source: Author 2020

FIGURE 3b
House C pictorial view
Source: Author 2020

The house was made of old galvanized sheet metal and had a lining of 3mm plywood board. The only exception in the house construction is the shower and w.c. cubicle that was made of stone masonry. The house had five windows on three of its four sides but only the window in the kitchen and shower/toilet cubicle were opened during the research data collection period. The roof design is a single slope roof with a fall towards the back side.

The house was studied in the state of its users' adaptation to their environment. The occupants woke up at 5am to shower and prepared breakfast at 6am; at 8am the front window would be opened but the outside door remained shut much of the time unless on a hot day when some of the occupants were in; all the occupants would be in the house by 7pm when preparation of supper was done using a two burner gas cooker and the cooking would be through by 8pm; the occupants would relax in the sitting area until about 11am when they would go to sleep; one occupant slept in the sitting area, two in bedroom 1 and their mother in bedroom 2.

(iii) House D

House D was a single room house occupied by a married couple who had no children. The house was made of new galvanized sheet metal and lined with three ply boards on the inside. The house had a door and window on the front wall and had a single slope roof with a fall to the back side (**Figures 4a** and **4b**).

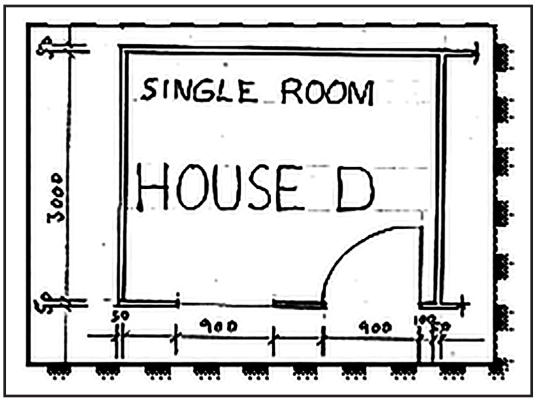

FIGURE 4a
House D layout plan
Source: Author 2020

FIGURE 4b
House D front view and back view
Source: Author 2020

The house was studied in the state of its users' adaptation to their environment. The occupants woke up at 5am, heated their bathing water, made breakfast at about 6am, left the house at 7am and came back at 6pm. Supper was prepared at 7pm using a kerosene stove and all activities would wind up at 9pm whereby the couple went to bed.

(iv) House E

House E was a two roomed house (**Figures 5a** and **5b**) occupied by two adults (mother and house help) and one child. The house was made of new galvanized sheet metal and lined with 3mm plywood boards on the inside. The house had one door and only two windows on the front wall. The roof was a single slope roof with a fall to the backside.

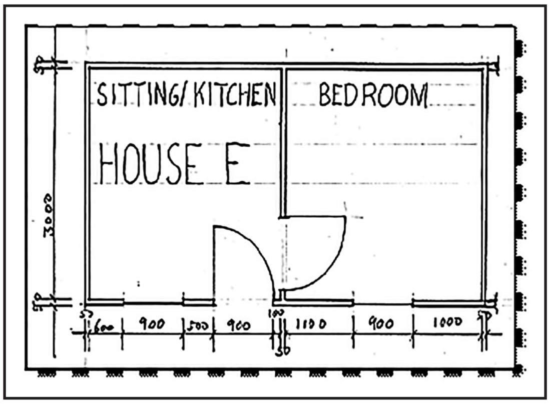

FIGURE 5a
House E layout plan
Source: Author 2020

FIGURE 5b
House E front view
Source: Author 2020

The house was studied in the state of its users' adaptation to their environment. The occupants woke up at 5am, heated bathing water, made breakfast at 6am and the mother would leave for work at 7am while the househelp remained with the child and they spent much of their time outside while the house remained closed with only the sitting room window open. The mother would be back at 6pm and supper would be prepared at 7pm using a gas stove. All activities would end at 9pm and the house occupants would relax up to about 11pm when they would all go to sleep.

(b) Observed thermal characteristics of the case study buildings

The thermal mass of the building is low as observations showed the building's internal thermal environment responded almost instantaneously to external downward temperature drop or upward temperature rise (**Figure 6**).

(c) Buildings' thermal conditions

(i) Influence of occupants on the buildings' thermal conditions

From the observation results in **Figure 7**, it is notable that cooking methods used by occupants of House B greatly vary their thermal conditions as compared to the empty House A.

(ii) Online compliance check of the research buildings' thermal conditions

Compliance was checked using the CBC Thermal Comfort Tool for ASHRAE-55 (adoptive method).

House A operative temperature (May) = 20.2°C and outdoor temperature 18.3°C complies with ASHRAE Standard 55-2017.

- 80% acceptable limits = Operative temperature 20.0 to 27.0°C (comfortable)
- 90% acceptable limits = Operative temperature 21.0 to 26.0°C (too cool) (**Figure 8**)

House B operative temperature (May) = 24.2°C and outdoor temperature 18.3°C complies with ASHRAE Standard 55-2017.

- 80% acceptable limits = Operative temperature 20.0 to 27.0°C (comfortable)
- 90% acceptable limits = Operative temperature 21.0 to 26.0°C (comfortable)

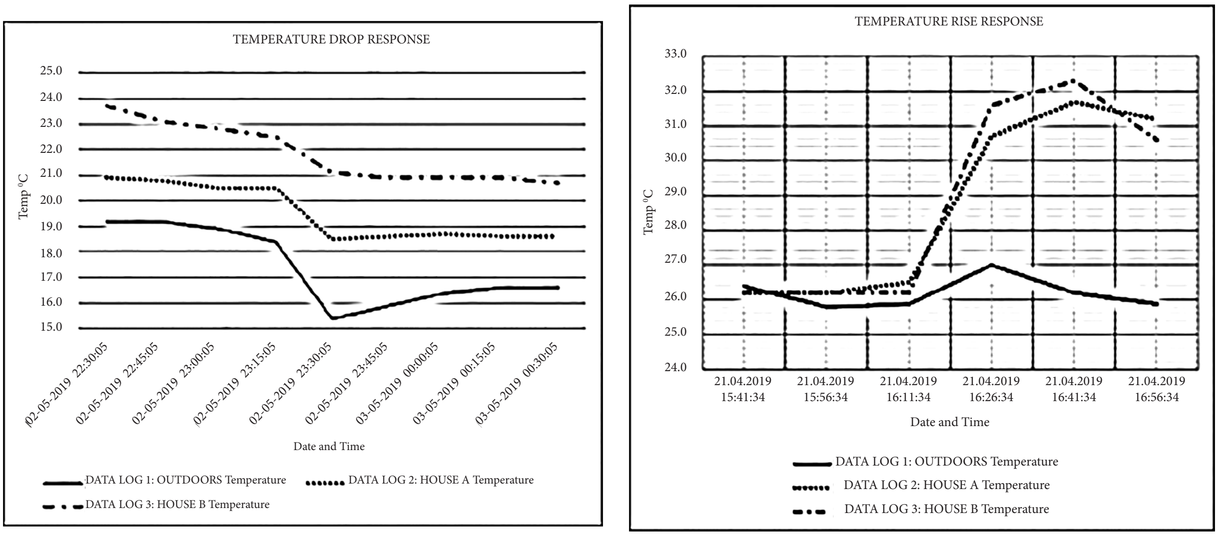

FIGURE 6
Temperature drop and rise response
Source: Author 2020

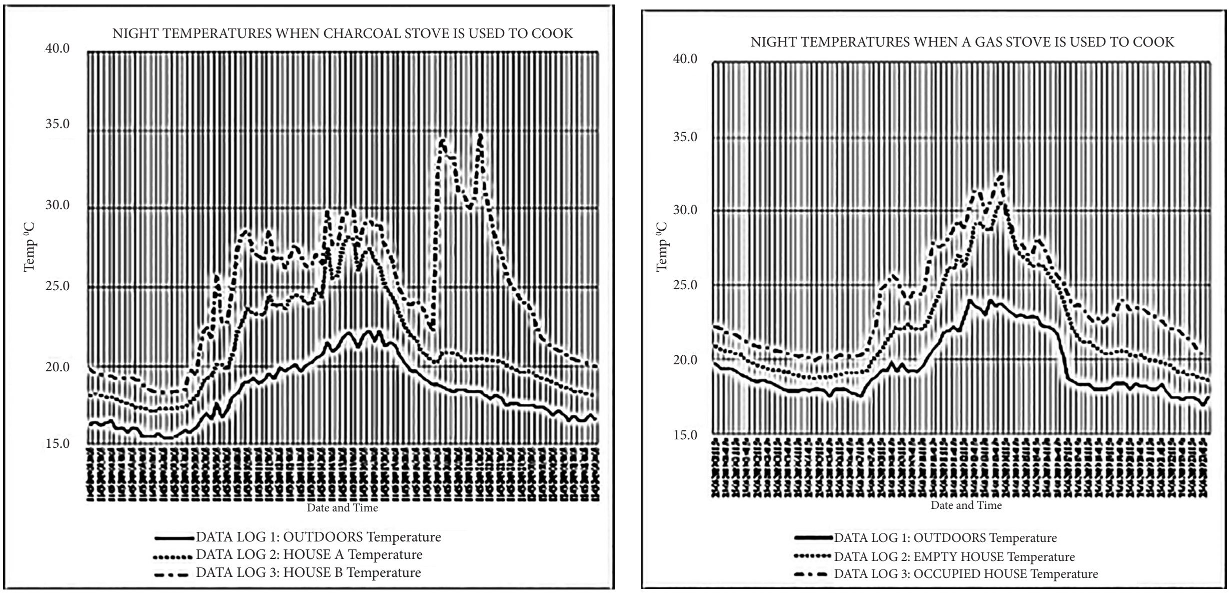

FIGURE 7
Method of cooking effects on internal temperatures
Source: Author 2020

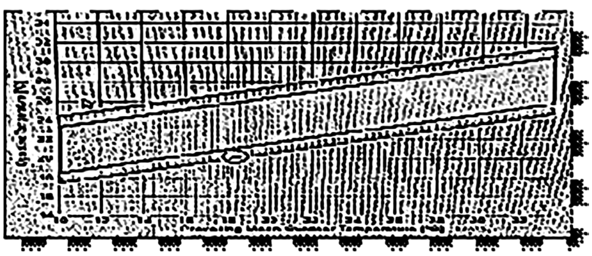

FIGURE 8
Adoptive chart for House A (May)
Source: Author 2020

House B operative temperature (July) = 22.5°C and outdoor temperature 18.1°C complies with ASHRAE Standard 55-2017.

- 80% acceptable limits = Operative temperature 19.9 to 26.9°C (comfortable)
- 90% acceptable limits = Operative temperature 20.9 to 25.9°C (comfortable)

House B operative temperature (Aug) = 20.0°C and outdoor temperature 18.3°C complies with ASHRAE Standard 55-2017.

- 80% acceptable limits = Operative temperature 20.0 to 27.0°C (comfortable)

- 90% acceptable limits = Operative temperature 21.0 to 26.0°C (comfortable)

House C operative temperature (July) = 23.6°C and outdoor temperature 18.1°C complies with ASHRAE Standard 55-2017.

- 80% acceptable limits = Operative temperature 19.9 to 26.9°C (comfortable)

- 90% acceptable limits = Operative temperature 20.9 to 25.9°C (comfortable) (**Figure 9**)

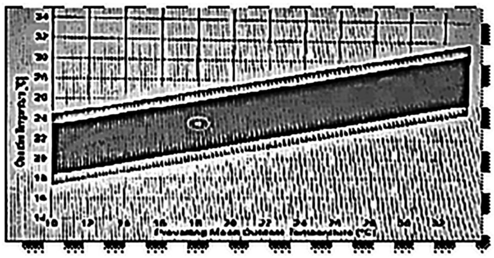

FIGURE 9
Adoptive chart for House C (July)
Source: Author 2020

House C operative temperature (Aug) = 23.4°C and outdoor temperature 18.3°C complies with ASHRAE Standard 55-2017.

- 80% acceptable limits = Operative temperature 20.0 to 27.0°C (comfortable)

- 90% acceptable limits = Operative temperature 21.0 to 26.0°C (comfortable)

House D operative temperature (Oct) = 21.1°C and outdoor temperature 18.0°C complies with ASHRAE Standard 55-2017.

- 80% acceptable limits = Operative temperature 19.9 to 26.9°C (comfortable)

- 90% acceptable limits = Operative temperature 20.9 to 25.9°C (comfortable)

House E operative temperature (Oct) = 26.8°C and outdoor temperature 18.0°C complies with ASHRAE Standard 55-2017.

- 80% acceptable limits = Operative temperature 19.9 to 26.9°C (comfortable)

- 90% acceptable limits = Operative temperature 20.9 to 25.9°C (too warm) (**Figure 10**)

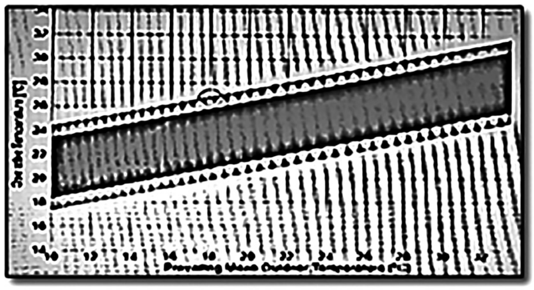

FIGURE 10
Adoptive chart for House E
Source: Author 2020

(d) Humidity levels and condensation risk

(i) Relative humidity levels of the houses

May 2019, empty house (House A) and occupied house (House B)

The regression relationship of the outdoors relative humidity with that in House A (**Figure 11**) showed a high positive correlation of the two measured variables; the coefficient of determination (R^2) is 0.9746, meaning the total proportion in the internal relative humidity levels of the empty house (House A) which is accounted for by the linear variation of the outdoors relative humidity is 97.46%.

Likewise, **Figure 12** shows high positive correlation of the two measured variables; the coefficient of determination (R^2) is 0.9359, meaning the total proportion in the internal relative humidity levels in the occupied house (House B) which is accounted for by the linear variation of the outdoors relative humidity is 93.59%.

From the comparison of the two results it can be shown that the relative humidity of House B has a lower correlation than of House A, hence it can be deduced that the internal relative humidity levels

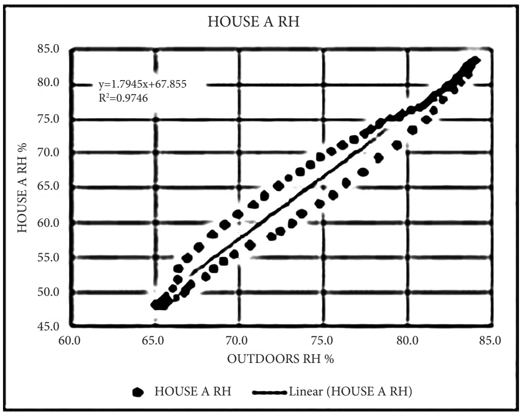

FIGURE 11
House A relative humidity regression analysis
Source: Author 2020

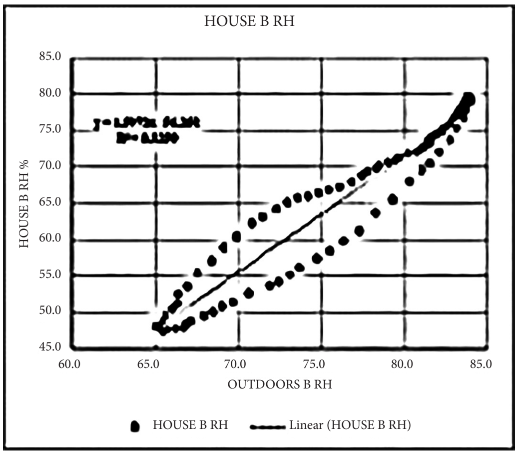

FIGURE 12
House B relative humidity regression analysis
Source: Author 2020

of an occupied sheet metal clad residential building is less influenced by the external environment's relative humidity as compared to an empty sheet metal clad building of the same size. At over 90% for both houses, their internal relative humidity levels are heavily influenced by their external environment's relative humidity.

(ii) Absolute humidity (AH) levels of the houses

May 2019, Empty house (House A) and occupied house (House B)

Equation 1 was used to convert relative humidity using temperatures from May 2019 data into absolute humidity values. As shown in **Figure 13**, the regression relationship of the outdoors absolute humidity with that in House A presented a low positive correlation of the two measured variables; the coefficient of determination (R^2) is 0.5593; meaning the total proportion in the internal absolute humidity levels of the empty house (House A) which is accounted for by the linear variation of the outdoors absolute humidity is just 55.93%.

Likewise, **Figure 14** shows low positive correlation of the two measured variables; the coefficient of determination (R^2) is 0.4902; meaning that the total proportion in the internal absolute humidity levels in the occupied house (House B) which is accounted for by the linear variation of outdoors absolute humidity is just 49.02%.

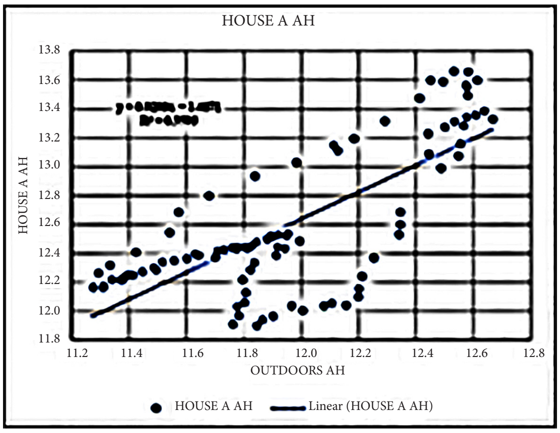

FIGURE 13
House A absolute humidity regression analysis
Source: Author 2020

FIGURE 14
House B absolute humidity regression analysis
Source: Author 2020

From the comparison of the two results it can be shown that the absolute humidity of House B has a lower correlation than of House A, hence it can be deduced that the internal absolute humidity levels of an occupied sheet metal clad residential building is less influenced by the external environment as compared to an empty sheet metal clad building of the same size. At about 50% for both houses, their internal absolute humidity levels are slightly influenced by their external environments. This is likely to be attributed to poor ventilation of the buildings, also there being other sources of moisture in the buildings such as that rising out of the floors and that from presence of occupants with their activities (cooking and body perspiration). It was also noted that the AH levels of House A between 3pm and 6pm drop to the same level as the outdoors AH (**Figure 15**). This is likely to be attributed to there being no resistance to the warm air movements in the empty house as it escapes through the top of the building by convention and is replaced by cooler air from outside.

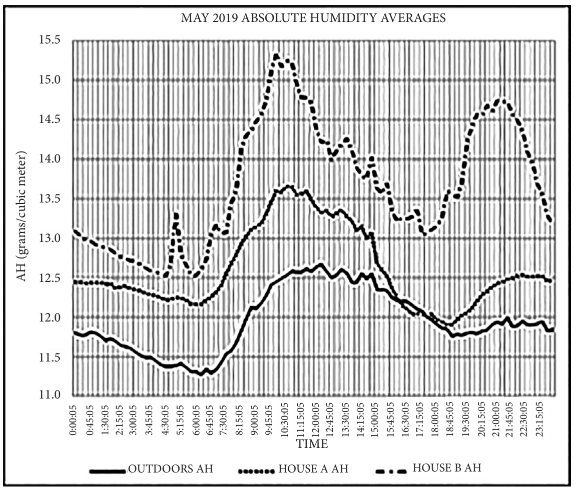

FIGURE 15
May 2019 absolute humidity levels
Source: Author 2020

July 2019 House B and C absolute humidity levels

As shown in **Figure 16**, both houses maintain higher levels AH than the external environment confirming that there is poor ventilation as the occupants lock themselves up in during the cold month of July.

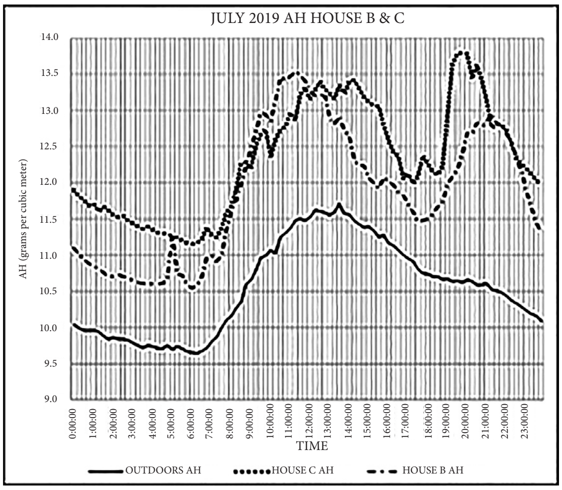

FIGURE 16
July 2019 absolute humidity levels
Source: Author 2020

August 2019 House B and C absolute humidity levels

Figure 17 shows that the difference in the AH levels indoors from those of outdoors is a function of how effective the ventilation of the sheet metal clad building is. House B which is not sealed tends to balance its AH levels with those of outdoors between 3pm and 6pm when the doors and windows are open showing the ventilation is effective at that moment. House C which is sealed maintains high levels of AH despite the windows being open hence showing that its ventilation is not effective.

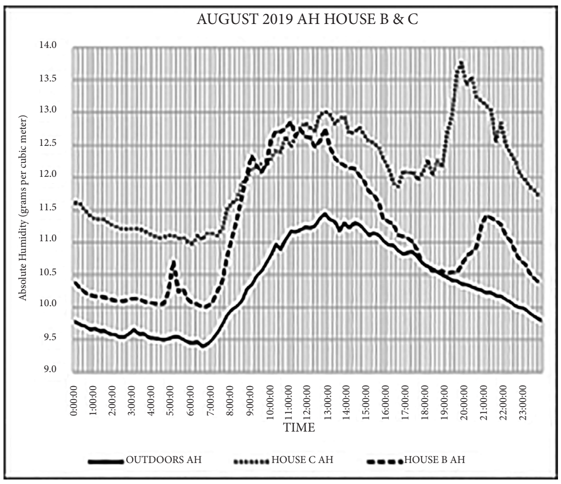

FIGURE 17
August 2019 absolute humidity levels
Source: Author 2020

October 2019 House D and E absolute humidity levels

From the **Figure 18**, House D and E (which are sealed) have poor ventilation as at no time does their AH values approach those of outdoors.

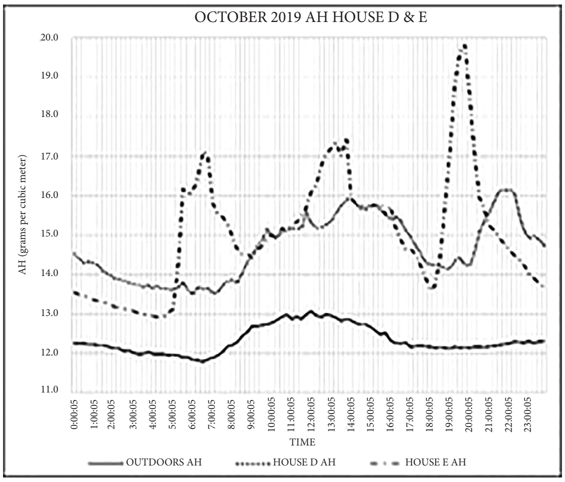

FIGURE 18
October 2019 absolute humidity levels
Source: Author 2020

(ii) Dew point temperatures

By using **Equation 2**, the dew point temperatures were calculated and graphs plotted for Houses A, B, C, D and E.

May 2019, House A and B

From May 2019 data (with average monthly temperature of 18.3°C), House A which was vacant showed no signs of being at risk of condensation forming as the outdoors temperatures do not drop below the internal dew point (**Figure 19**).

House B data analysis for May 2019 (**Figure 20**) with an average monthly temperature of 18.3°C, shows the house to be at risk of temporary condensation formation between 9am and 10am (porridge is cooked for toddlers at that time). There is also a rise in the dew point temperatures in the house between 7pm and 10pm (corresponding to cooking of evening meals) which raises the risk of condensation formation.

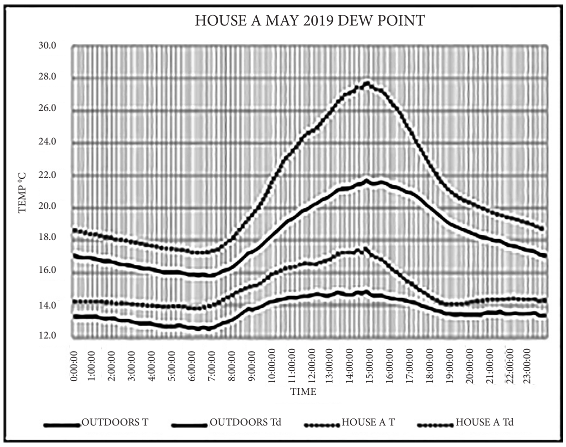

FIGURE 19
May 2019, House A dew point
Source: Author 2020

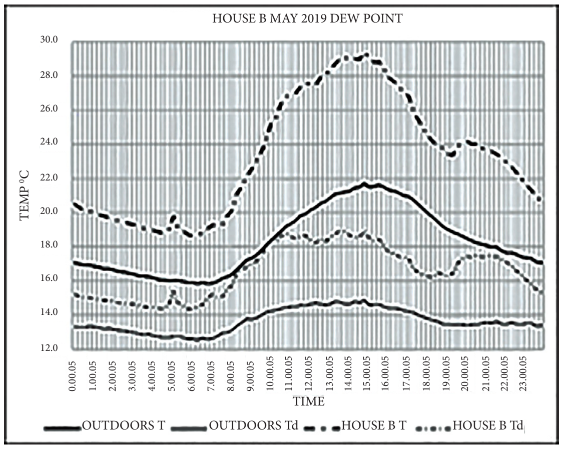

FIGURE 20
May 2019, House B dew point
Source: Author 2020

July 2019 House B and C

House B data analysis for July 2019 (**Figure 21**) with an average monthly temperature of 17.4°C, shows that the house is at less risk of condensation forming when the overall average environment was much colder in the month of July 2019 than what was seen in the warmer month of May 2019.

House C data analysis for July 2019 (**Figure 22**) shows the house to be at less risk of condensation in the cold month of July (average temperature 17.4°C).

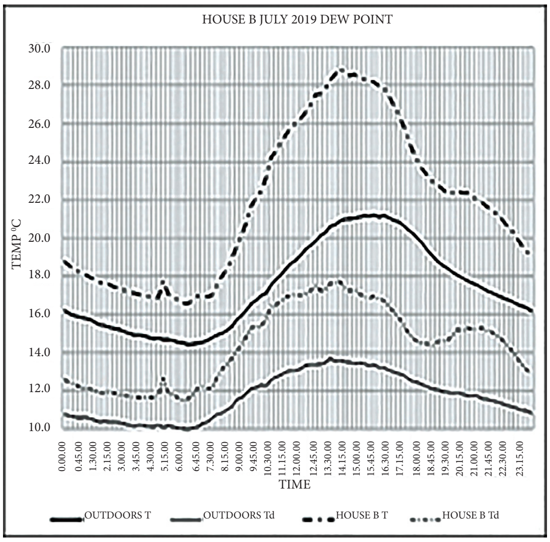

FIGURE 21
July 2019, House B dew point
Source: Author 2020

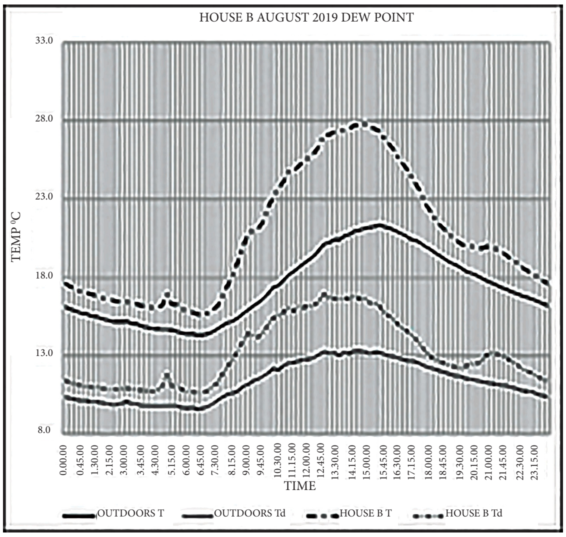

FIGURE 23
August 2019, House B dew point
Source: Author 2020

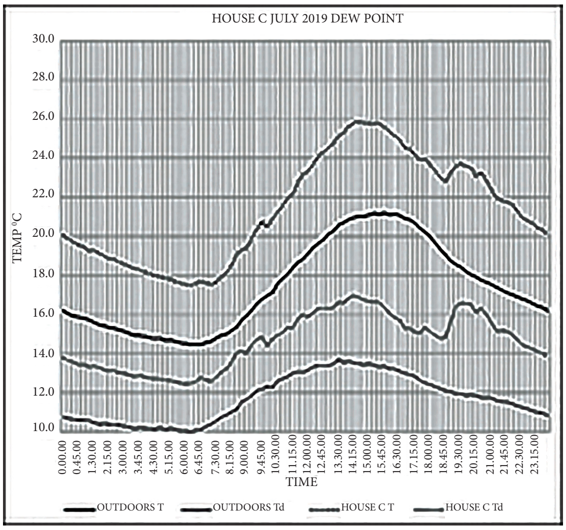

FIGURE 22
July 2019, House C dew point
Source: Author 2020

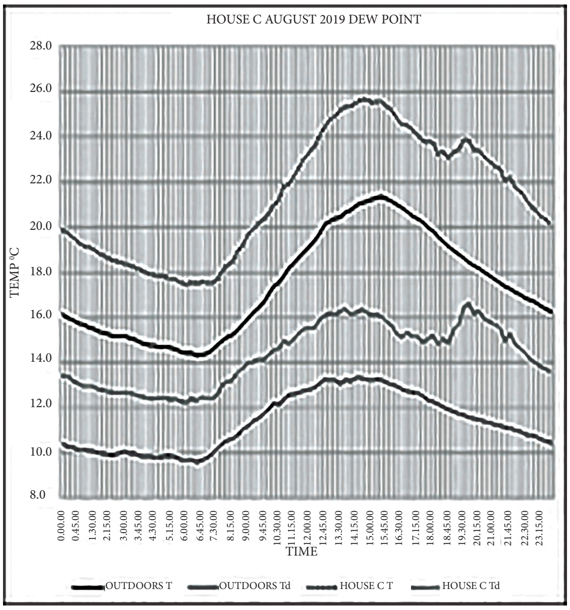

FIGURE 24
August 2019, House C dew point
Source: Author 2020

August 2019 House B and C

House B data analysis for August 2019 (**Figure 23**) with an average monthly temperature of 17.4°C, shows that the house is at less risk of condensation forming on internal side of walls.

House C data analysis for August 2019 (**Figure 24**) with an average monthly temperature of 17.4°C, shows that the house is at less risk of condensation forming in the cold month of August.

October 2019 House D and E

House D data analysis for October 2019 whose average monthly outdoor temperature was 18.1°C (**Figure 25**) shows the house to be at a high risk of condensation forming on its walls as the outdoors temperatures drop below the internal dew point temperatures at night.

House E data analysis for October 2019 (**Figure 26**) with an average monthly temperature of 18.1°C, shows that the house is at a high risk of condensation forming on the internal side of the external walls at times of heightened internal activities i.e. between 5am and 9am, which was heating bathing water and breakfast preparation while between 7pm and 9pm was supper preparation.

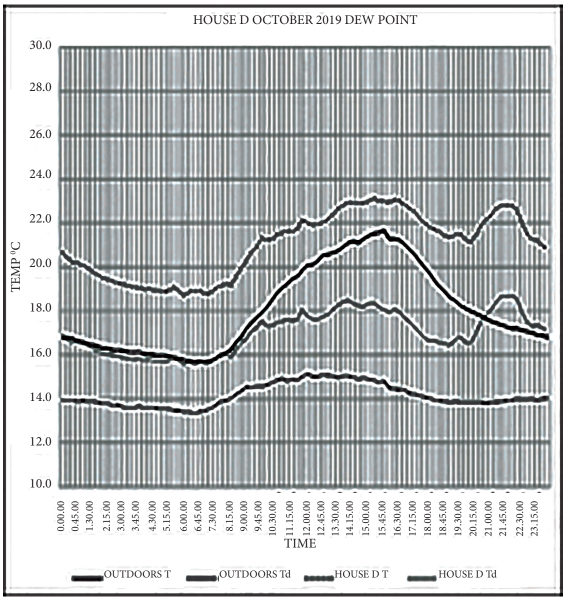

FIGURE 25
October 2019, House D dew point
Source: Author 2020

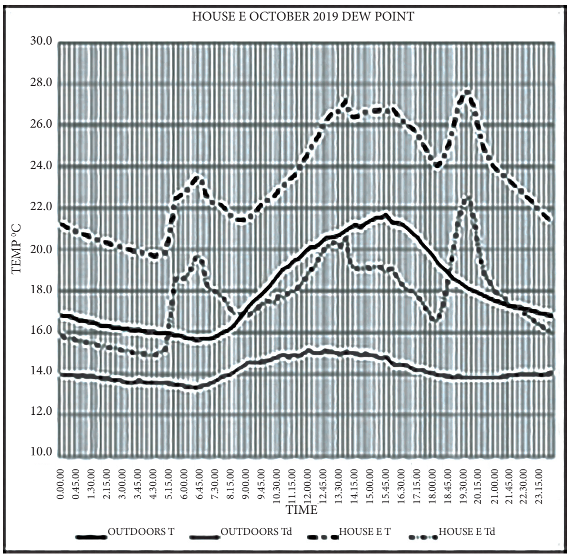

FIGURE 26
October 2019, House E dew point
Source: Author 2020

(e) 24-hour micro-climate predicting model

(i) Regression analysis and simulation model derivation

The daily hourly temperatures were recorded (**Figure 27**) from outdoors; House A and House B were averaged to come up with the daily average temperatures (**Figure 28**) for May 2019.

From the daily average temperatures of May 2019, linear regression analysis was done separately for each house (House A and House B) to determine the relationship of their internal thermal environments to that of their external environment. From the Model As regression derivation for House A regression Model A linear; it showed a high positive correlation of the two measured variables; the coefficient of determination (R^2) is 0.9626, meaning that the total proportion in the internal thermal conditions in the empty house which is accounted for by the linear variation of the ambient temperature is 96.26%. Likewise Model Bs regression derivation for House B regression Model B linear; it showed high positive correlation of the two measured variables; the coefficient of determination (R^2) is 0.9388, meaning that the total proportion in the internal thermal conditions in the occupied house which is accounted for by the linear variation of the ambient temperature is 93.88%. From the comparison of the two results it can be seen that the data from the House B has a lower correlation than that of House A hence it can be deduced that the internal thermal conditions of an occupied sheet metal clad residential building is less influenced by the external environment as compared to an empty sheet metal clad building of the same size. At over 90% for both houses, their internal thermal conditions are heavily influenced by their external environments.

Using the May 2019 average daily temperatures, regression analysis was used to derive two sets of regression models (Model As from House A data and Model Bs from House B data.

(ii) Validation and accuracy check of derived regression curve models

July 2019 temperature data for House B and C was used to validate regression Model As and

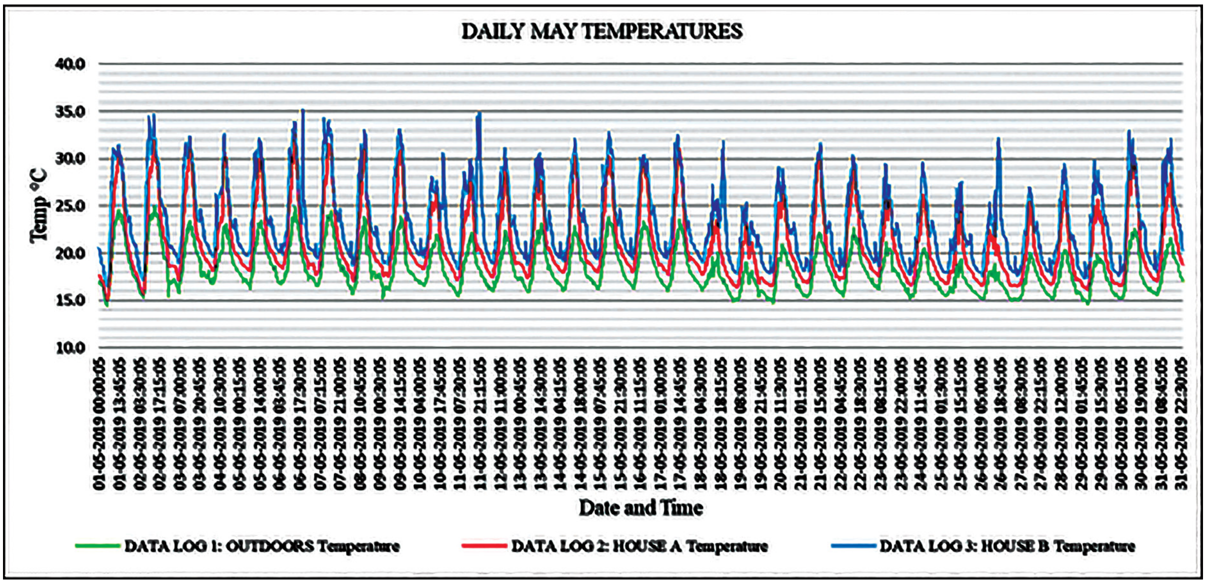

FIGURE 27
Daily temperatures of May 2019
Source: Author 2020

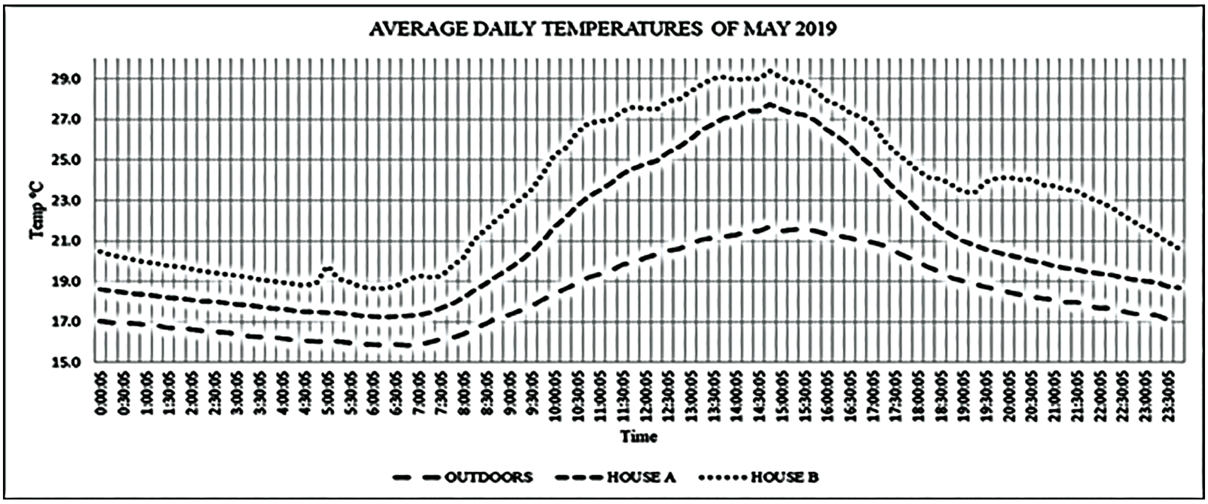

FIGURE 28
Average daily temperatures of May 2019
Source: Author 2020

Model Bs whereby the model that gave the closest predictions to the actual temperatures recorded was chosen and those that gave unrealistic figures were discarded. The results are summarized in **Tables 1**, **2**, **3** and **4**.

The best model was from Model B, House C, a polynomial 3 function with an accuracy of 97.56% giving the model equation for predicting the 24-hour internal thermal conditions in sheet metal clad residential buildings for any outdoor temperature as shown in **Equation 3**.

Equation 3:

$$T_i = 0.0119T_o^3 - 0.7711T_o^2 + 18.058T_o - 121.53$$

Where; T_i *is the indoor temperature.*

T_o *is the outdoors temperature.*

TABLE 1: Models A, House B

Model Type	R^2	Prediction Accuracy
Linear	0.9395	93.95%
Exponential	0.9298	92.98%
Logarithmic	0.9409	94.09%
Polynomial 2	0.9063	90.63%
Polynomial 3	0.9132	91.32%
Polynomial 4	0.8879	88.79%
Power	0.9372	93.72%

Source: Author 2020

TABLE 2: Models A, House C

Model Type	R^2	Prediction Accuracy
Linear	0.9644	96.44%
Exponential	0.9457	94.57%
Logarithmic	0.9723	97.23%
Polynomial 2	0.9113	91.13%
Polynomial 3	0.9216	92.16%
Polynomial 4	0.8842	88.42%
Power	0.9590	95.90%

Source: Author 2020

TABLE 3: Models B, House B

Model Type	R^2	Prediction Accuracy
Linear	0.9395	93.95%
Exponential	0.9304	93.04%
Logarithmic	0.9409	94.09%
Polynomial 2	0.9384	93.84%
Polynomial 3	0.9349	93.49%
Polynomial 4	0.6807	68.07%
Power	0.9376	93.76%

Source: Author 2020

(iii) Validation of the 24-hour micro-climate predicting model

Equation 3 was then validated with data for August 2019 (House B & C) and October 2019 (House D & E). The equation predicted the internal thermal conditions as shown in **Figures 29** and **30**.

From the above validation results, the micro-climate prediction model is able to predict the internal thermal environment of sheet metal clad buildings of low insulation with over 60% accuracy. It is also notable from the prediction results of House E that a house with poor ventilation and high activity levels is less predictable by the model.

TABLE 4: Models B, House C

Model Type	R^2	Prediction Accuracy
Linear	0.9644	96.44%
Exponential	0.9468	94.68%
Logarithmic	0.9723	97.23%
Polynomial 2	0.9750	97.50%
Polynomial 3	0.9756	97.56%
Polynomial 4	0.6456	64.56%
Power	0.9597	95.97%

Source: Author 2020

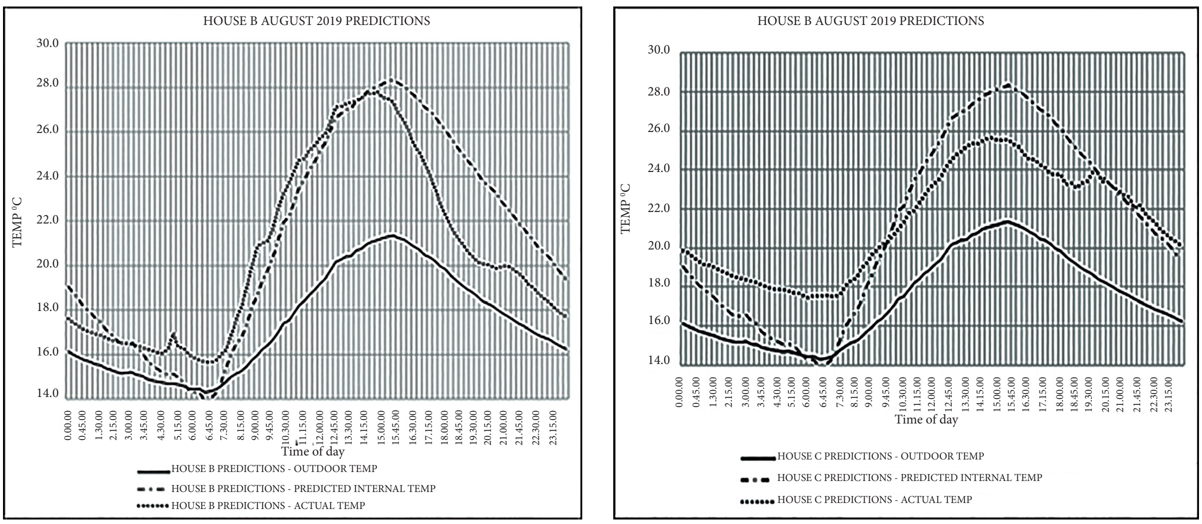

FIGURE 29
House B & C August prediction at 84.87% & 98.03% accuracy respectively
Source: Author 2020

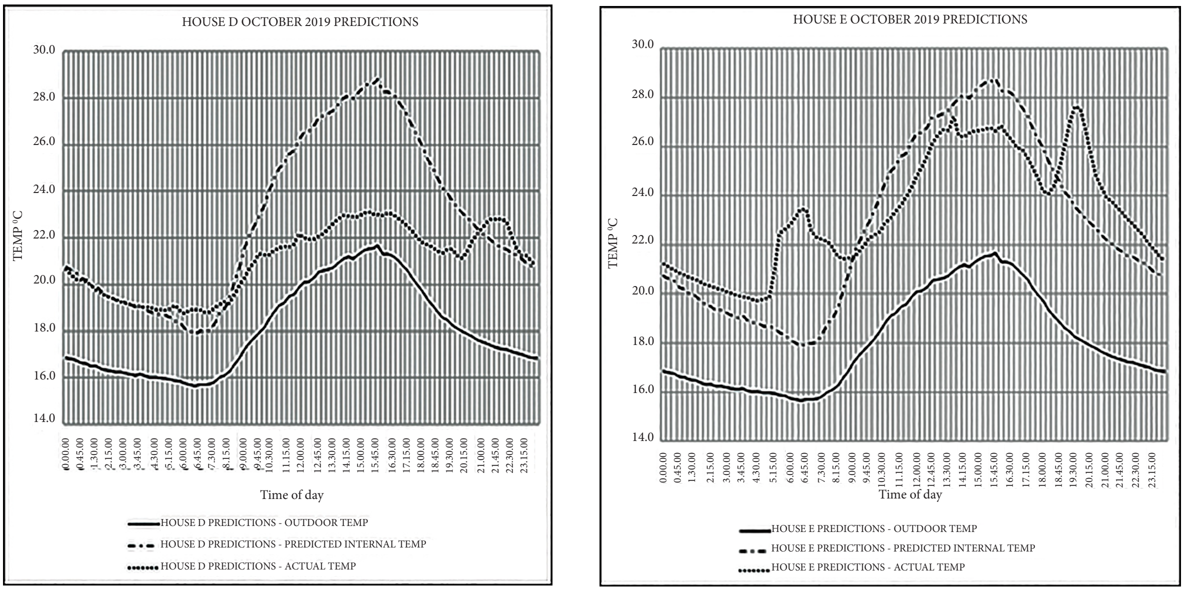

FIGURE 30
House D & E October prediction at 79.00% & 69.13% accuracy respectively
Source: Author 2020

CONCLUSION

The following conclusions have been drawn from the research:

(a) Under normal use, the thermal conditions in an occupied sheet metal clad residential building can comply with the ASHRAE Standard 55-2017 (ignoring the heating effects of cooking activities).

(b) Sheet metal clad residential buildings can be at risk of temporary condensation forming during the warm months of the year than during the cold months of the year. The buildings with poor ventilation were at highest risk than those with effective ventilation.

(c) The micro-climate predicting model can predict the internal thermal conditions of any sheet metal clad residential building using the outdoor temperatures. The model has a higher prediction accuracy with buildings of moderate to good ventilation than those with poor ventilation.

RECOMMENDATIONS

(a)The investigation of internal thermal conditions in sheet metal clad residential buildings should be extended to other parts of Kenya so as to establish the suitability of sheet metal clad residential buildings as accommodation in the different climatic zones. A standard setting the internal thermal conditions for different types of buildings in Kenya should be developed.

(b) The ventilation size and positioning in sheet metal clad residential buildings should be designed to allow cross ventilation to reduce the risk of internal condensation formation.

(c) The Building Code of Kenya should be revised so as to recognize sheet metal clad buildings as reasonable structures for accommodating people.

CITED REFERENCES

Abrasheva, G., Senk, D. & Häußling, R. (2012). Shipping containers for a sustainable habitat perspective. *Revenue De Métallurgie.* 381-389.

Bolton, D. (1980). *The Computation of Equivalent Potential Temperature.* Imperial College. London: Atmospheric Physics Group.

Dear, R.D., Foo, S.C. & Leow, K.G. (1991). Thermal comfort in the humid tropics: Field experiments in air conditioned and naturally ventilated buildings in Singapore. *International Journal of Biometeorology.* 34, 259-265. doi:10.1007/BF01041840.

Han, J., Zhang, G., Zhang, Q., Zhang, J., Liu, J., Tian, L., ... Moschandreas, D.J. (2007). Field Study on Occupants' Thermal Comfort and Residential Thermal Environment in a Hot-humid Climate of China. *Building and Environment*. 4043-4050.

Kariuki, R.N., Mugwima, B.N... (2018). Effect of Walling Materials' Thermal Transmittance and Thermal Mass on Indoor Thermal Comfort in Nairobi. *Africa Habitat Review*. 1247-1262.

Lawrence, M.G. (2005). The relationship between relative humidity and the dew point temperature in moist air: A simple conversion and applications. *New York: Bulletin of the American Meteorological Society*. 86(2). doi:10.1175/BAMS-86-2-225.

Levinson, R., Akbari, H. & Berdahl, P. (2010). Measuring solar reflectance- Part I: Defining a metric that accurately predicts solar heat gain. *Solar Energy*. 84(9):1717-1744.

Okamoto-Mizuno, K., Mizuno, K., Michie, S., Maeda, A. & Iizuka, S. (1999). Effects of humid heat exposure on human sleep stages and body temperature. *SLEEP*. 767-773.

Real, S., Gomes, M.G., Bogas, J.A. & Ferrer, B. (2016, January 5). Thermal Conductivity of Structural Lightweight Aggregate Concrete. *Magazine of Concrete Research*. 1-12. doi:10.1680/jmacr.15.00424.

Republic of Kenya. (2016). *Housing Situation In Kenya.* Nairobi: Government Printers.

Schiavon, S., Hoyt, T. & Piccioli, A. (2019, August 01). Web application for thermal comfort visualization and calculation according to ASHRAE Standard 55. *Building Simulation*. 1-21. doi:10.1007/s12273-013-0162-3.

Suehrcke, H., Peterson, E.L. & Selby, N. (2008). Effect of roof solar reflectance on the building heat gain in a hot climate. *Energy and Buildings*. 2224-2235.